Supplementary Information for "Membrane tubulation by spherical nanoparticles: Effect of lateral tension"

Thomas R. Weikl

Energy minimization methods

To determine the minimum-energy shapes of the rotationally symmetric membranes around individually wrapped particles or cooperatively wrapped linear chains of particles, we extend the methodology of Ref. 1 to membranes under tension. In this methodology, we discretize the profiles of the rotationally symmetric membrane shapes in two different parametrizations.

In parametrization 1, the rotationally symmetric membrane shapes are described by the function $r(z)$ where z is the coordinate along the axis of rotation, and r is the radial distance from this axis. In this parametrization, the bending energy $E_{\rm be}$, membrane area A, and adhesion energy $E_{\rm ad}$ can be expressed as

$$E_{\rm be} = \int e_{\rm be}(z)\mathrm{d}z = \int \pi\kappa \frac{\left(r(z)r''(z) - r'(z)^2 - 1\right)^2}{r(z)\left(r'(z)^2+1\right)^{5/2}}\mathrm{d}z \quad (1)$$

$$A = \int a(z)\mathrm{d}z = \int 2\pi r(z)\sqrt{1+r'(z)^2}\mathrm{d}z \quad (2)$$

$$E_{\rm ad} = \int e_{\rm ad}(z)\mathrm{d}z = \int 2\pi \sum_{i=1}^{n_p} V(l_i) r(z)\sqrt{1+r'(z)^2}\mathrm{d}z \quad (3)$$

with $l_i = l_i(z, r(z))$ and the bending energy density $e_{\rm be}(z)$, area density $a(z)$, and adhesion energy density $e_{\rm ad}(z)$. Here, primes indicate derivatives with respect to z, and n_p is the number of considered particles, which are centered along the z-axis. For a membrane segment adhering at preferred separation l_o to a particle centered at $z = 0$, the membrane profile is $r = \sqrt{r_m^2 - z^2}$, and the densities are $e_{\rm be}(z) = 4\pi\kappa/r_m$, $a(z) = 2\pi r_m$, and $e_{\rm ad}(z) = -2\pi r_m U$, which are constant functions independent of z. If the particle is fully wrapped by the membrane from $z = -r_m$ to $z = r_m$, these densities lead to $E_{\rm be} = \int_{-r_m}^{r_m}(4\pi\kappa/r_m)\mathrm{d}z = 8\pi\kappa$, $A = \int_{-r_m}^{r_m} 2\pi r_m \mathrm{d}z = 4\pi r_m^2$, and $E_{\rm ad} = -\int_{-r_m}^{r_m} 2\pi r_m U \mathrm{d}z = -4\pi r_m^2 U$ as expected (see main text).

We use parametrization 1 to determine the membrane shapes around central particles in membrane tubules with distance $d \geq 2r_p$ between the particles. Because of the periodicity of the tubular shapes (see Fig. 2), we determine the minimum energy shape of a membrane segment from the center of a particle to the center of the membrane neck that connects to the neighbouring particle in the tubule. We discretize the membrane profile $r(z)$ of this membrane segment using 400 discretization points, express the derivates $r'(z)$ and $r''(z)$ as standard finite differences, and minimize the total energy E with respect to the radial distances $r(z_i)$ at the discretization points z_i and with respect to the distance d of particles using the software Mathematica 14.3[2]. The number of particles in this minimization is $n_p = 2$, because only the two particles connected by the membrane neck of the segment contribute to the adhesion energy of the segment. For central particles in the tubule, the excess area ΔA of the membrane segments wrapping these particles relative to the planar membrane prior to tubule formation is equal to the area A of the segments.

We also use parametrization 1 to determine the rotationally symmetric membrane shape around a single, deeply wrapped particle, e.g. the left shape of Fig. 2. A complication here is that the derivative $r'(z)$ diverges at the membrane point on the symmetry axis, i.e. the point at the bottom of the left shape of Fig. 2, and when the non-adhering membrane approaches the surrounding planar membrane. The divergence of $r'(z)$ at the membrane point on the symmetry axis can be treated by taking into account that the energy densities $e_{\rm be}(z)$, $e_{\rm ad}(z)$ and $\tau a(z)$ are constant functions for the adhering membrane segment with spherical membrane shape (see above). The divergence of $r'(z)$ as the non-adhering membrane approaches the surrounding planar membrane, in contrast, is unproblematic only in the case of zero membrane tension, because the non-adhering membrane then adopts a catenoidal shape with zero total energy because the bending energy of the catenoid is zero. For tensionless membranes, the membrane profile therefore just needs to be determined up to a discretization point z_n of the non-adhering membrane at which the total energy is zero[1]. For membranes with finite tension, we numerically determine the membrane profile also up to a discretization point z_n of the non-adhering membrane around a single deeply wrapped particle at which the slope $r'(z_n)$ still allows a reliable numerical determination of the total energy. For z values beyond this point, we use the analytical solution $z(r) = z_o + cK_o(r\sqrt{\kappa/\tau})$ with Bessel function K_o for rotationally symmetric membrane shapes with small gradients $z'(r)$[3], which we fit to the last 20 points of the numerically determined profile until point z_n. For values of the rescaled tension γ up to 1, the analytical continuation of the non-adhering membrane shape contributes only marginally to the total energy. For $\gamma = 1$, this contribution is about 0.05 κ for parameters of Fig. 4. For the values $\gamma = 2$ and 5 considered in Fig. S1, however, the analytical continuation of the non-adhering membrane contributes about 0.1 κ and 0.25 κ to the total energy, respectively. This tension-induced increase in the elastic energy of the non-adhering membrane around a single particle leads to an increase of the energy gain ΔE for the cooperative wrapping in tubules at sufficiently large rescaled adhesion energies u (see Fig. S1(b)). In the numerical minimization of the total energy of the discretized membrane profile, we use a discretization length $\delta z = r_m/400$ and up to a total of 1000 discretization points, depending on the location of the point z_n. The excess area of the discretized membrane up to z_n is determined as $\Delta A = A - 2\pi r(z_n)^2$ with area A calculated based on Eq. (2). To determine the transition values u_t of the discontinu-

Max Planck Institute of Colloids and Interfaces, Department of Biomolecular Systems, Potsdam Germany. E-mail: thomas.weikl@mpikg.mpg.de

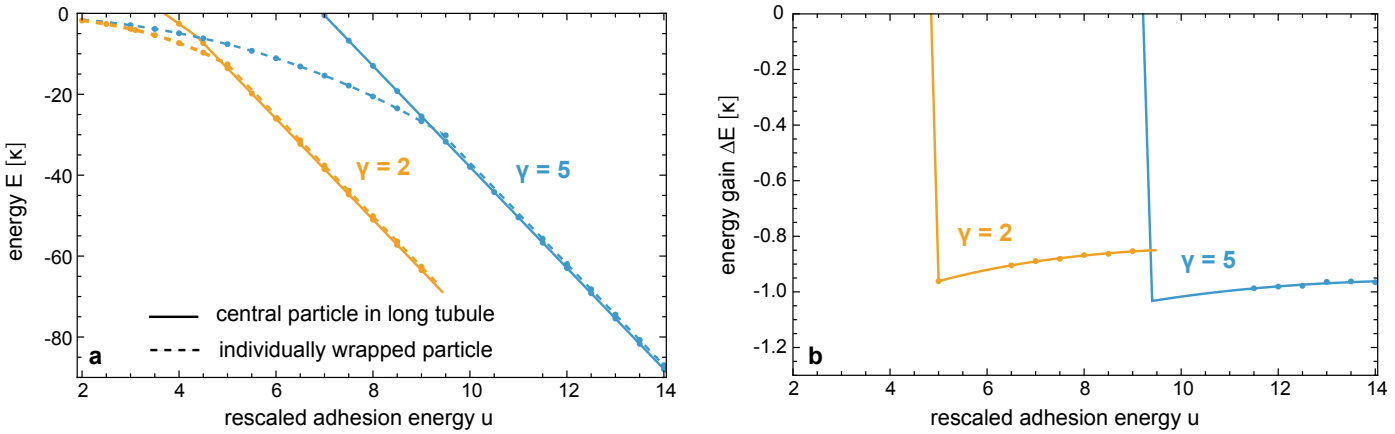

Fig. S1 (a) Total energy E of individually wrapped particles (points interpolated by dashed lines) and per central particle in long membrane tubules wrapping many particles (points interpolated by full lines) versus rescaled adhesion u at the high rescaled tension values $\gamma = 2$ and 5 for the same parameter values as in Figs. 3 and 4. (b) Energy gain ΔE per central particle in long membrane tubule relative to an individually wrapped particle versus rescaled adhesion energy u at $\gamma = 2$ and 5.

ous transition from weakly undulated to deeply undulated tubule shapes at the rescaled tension values $\gamma = 0.5$ and 1 in Fig. 3, minimizations for values of u in the vicinity of u_t are started both from weakly undulated and deeply undulated tubule shapes to identify the stable minimum-energy state.

To determine the rotationally symmetric membrane shape around particles that are less than half-wrapped by the membrane, we use parametrization 2 in which the membrane profile is described by the function $z(r)$. In this parameterization, the bending energy $E_{\rm be}$, excess area ΔA, and adhesion energy $E_{\rm ad}$ can be expressed as

$$E_{\rm be} = \int \pi\kappa \frac{(rz''(r)+z'(r)^3+z'(r))^2}{r(1+z'(r)^2)^{5/2}} {\rm d}r \qquad (4)$$

$$\Delta A = \int 2\pi r \left(\sqrt{1+z'(r)^2}-1\right) {\rm d}r \qquad (5)$$

$$E_{\rm ad} = \int 2\pi V(l) r \sqrt{1+z'(r)^2}\, {\rm d}r \qquad (6)$$

with $l = l(z(r), r)$. To numerically determine the membrane profile $z(r)$ by minimisation of the total energy, we use the discretization length $\delta r = r_m/400$ and up to 3000 discretization points in numerical minimizations with Mathematica 14.3.

Model parameters for tubulation by GEMs

In the artificial adhesion system previously presented and modelled in Ref. 4 (see Fig. 1d), a capsid particle with a radius of 15 nm is densely covered by 180 green fluorescent proteins (GFPs), which are connected by unstructured 12-residue peptide linkers to the capsid proteins, leading to a radius $r_p = 19$ nm of the GFP-covered particle. The GFPs bind to anti-GFP nanobodies attached to the cell membranes by glycosylphosphatidylinositol (GPI) anchors. Based on the dimensions and linker attachment sites of the GFP-nanobody complex and the flexibility of the linkers, which allow also for tilting of the complex, the adhesion potential was estimated as a Gaussian potential with standard deviation $\xi = 1$ nm and preferred binding separation $l_o = 8$ nm between capsid particle surface and membrane midplane[4]. A membrane vesicle wrapping a single particle thus has the radius $r_m = (15+8)$ nm $= 23$ nm. In this continuum modeling of particle adhesion, the adhesion energy per area[4]

$$U = \frac{k_B T}{A} \ln[[{\rm R}]/\eta {\rm K_d}] \qquad (7)$$

depends on the vesicle area per protein complex $A = 4\pi r_m^2/180 \simeq 37$ nm^2, the area concentration $[{\rm R}]$ of GPI-anchored nanobodies in the cell membrane, and the dissociation constant K_d of the GFP-nanobody complex. The parameter η in this equation is a "conversion length" from 3D binding of the soluble complex to the 2D binding of the anchored complex at the preferred separation l_o[5].

Energy densities

Fig. S2c compares the total energy densities e of a central particle in a tubule and of an individually wrapped particle for the rescaled adhesion energy $u = 5$ at the values 0, 0.2, 0.5, and 1 of the rescaled tension γ. The total energies E of Fig. 4a result from an integration of these energy densities (see above). As functions of the rescaled coordinate z/r_m, the total energy density of spherical membrane segments with radius r_m attains the constant values $e = -2\pi\kappa(3-\gamma)$ at $u = 5$. For individually wrapped particles centered at $z/r_m = 0$, the total energy densities in Fig. S2c (dashed lines) adopt this value in the adhering membrane segment from $z/r_m = -1$ to about $z/r_m = 0.5$. For a particle located at $z/r_m = 0$ in a membrane tubule, the total energy densities in Fig. S2c (full lines) are symmetric around $z/r_m = 0$ and adopt the value $e = -2\pi\kappa(3-\gamma)$ of a spherical membrane segment with radius r_m between about $z/r_m = -0.5$ and $z/r_m = 0.5$. For $z/r_m > 0.5$, the total energy densities of an individually wrapped particle and a central particle in a tubule are closely similar due to similar membrane shapes in the contact regions in which the membrane detaches from the particle and forms a neck (see Fig. S2a and b for exemplary membrane shape profiles at $\gamma = 0.5$). The total energy densities first slightly increase for $z/r_m > 0.5$, then adopt a minimum around $z/r_m = 0.9$, and finally attain a value of 0 for a tensionless membrane with $\gamma = 0$ or positive values for $\gamma > 0$ in the

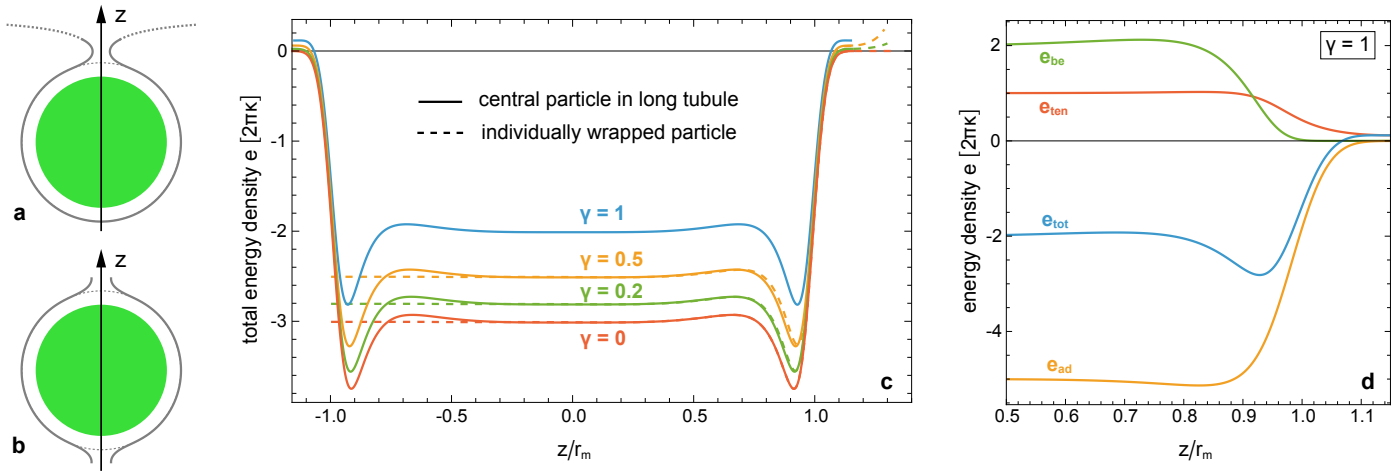

Fig. S2 Membrane shape profiles and energy densities at the rescaled adhesion energy $u = 5$. (a) Membrane shape profile for an individually wrapped particle and (b) membrane shape profile for a central particle in a tubule at the rescaled tension $\gamma = 0.5$. The dotted continuation of the membrane neck in (a) results from a fit of the analytical solution $z(r) = z_o + cK_o(r\sqrt{\kappa/\tau})$ of the shape equation for small gradients $z'(r)$ to the numerically determined shape (see Methods). The thin dashed lines in (a) and (b) represent a circle with membrane radius $r_m = 23$ nm. (c) Total energy densities e of a central particle in a tubule (full lines) and an individually wrapped particle (dashed lines) centered at $z = 0$ versus rescaled coordinate z/r_m at various values of the rescaled tension γ. (d) Bending energy density $e_{\rm be}$, adhesion energy density $e_{\rm ad}$, energy density $e_{\rm ten}$ associated with the membrane tension, and total energy density $e = e_{\rm be} + e_{\rm ten} + e_{\rm ad}$ of a central particle in a tubule for values of the rescaled coordinate $z/r_m \geq 0.5$ at the rescaled tension $\gamma = 1$. In adhering membrane segments with radius r_m, these energy densities attain the constant values $e_{\rm be} = 4\pi\kappa$, $e_{\rm ad} = -2\pi^2 {\rm U} = -2\pi\kappa{\rm u} = -10\pi\kappa$ for $u = 5$, $e_{\rm ten} = 2\pi r m^2 \tau = 2\pi\kappa\gamma = 2\pi\kappa$ for $\gamma = 1$, and $e = -4\pi\kappa$. In the contact region in which the membrane detaches from the particle, the total energy density e attains a minimum at about $z/r_m = 0.9$, because the bending energy density $e_{\rm be}$ drops to zero at smaller values of z/r_m than the adhesion energy density $e_{\rm ad}$. In the contact region, the membrane shape changes from the spherical shape of the adhering membrane segment with radius r_m to the catenoidal shape of the membrane neck with bending energy zero, but still gains adhesion energy because of the finite range of the Gaussian adhesion potential with standard deviation $\xi = 1$ nm. The shape profiles are not affected by the particle radius r_p and the minimum neck radius $r_n = 2.5$ nm because the particles are not in contact in the tubules and because the membrane necks are not yet closed at $u = 5$ (see Figs. 3c and d).

non-adhering membrane neck that connects the wrapped particle to the surrounding planar membrane or the neighbouring particle in the tubule. The energy densities in Fig. S2d show that the initial increase of the total energy density for $z/r_m > 0.5$ results from an increase in the bending energy density $e_{\rm be}$, which then drops to zero in the membrane neck, indicating that the neck attains a catenoidal shape even at the largest rescaled tension $\gamma = 1$ considered here. The adhesion energy density drops to zero at larger values of z/r_m than the bending energy density, which leads to the minimum of the total energy density in the contact region. The energy densities of Fig. S2 are not affected by the minimum neck radius $r_n = 2.5$ nm because the membrane necks are not yet fully closed at the rescaled adhesion energy $u = 5$ for the standard deviation $\xi = 1$ nm of the adhesion potential considered here.

An energy gain ΔE of cooperative wrapping in tubules implies that the total energy contribution of the contact region is favourable. For $\gamma = 0$, the energy densities for a central particle in a tubule and an individually wrapped particle are identical in the region $z/r_m > 0$ that includes the contact region of the individually wrapped particle and one of the contact regions of the particle in the tubule. The energy gain ΔE thus results from the differences in the total energy densities for $z/r_m < 0$. In this region, the individual particle is wrapped by a spherical membrane segment with radius r_m, with total energy contribution $\int_{-1}^{0} e\, {\rm d}z/r_m \simeq -6\pi\kappa$. For the central particle in the tubule, the total energy density for $z/r_m < 0$ is symmetric to the profile for $z/r_m > 0$ and contributes $\int_{-d/2r_m}^{0} e\, {\rm d}z/r_m \simeq -19.50\kappa$, which is smaller than $-6\pi\kappa$ and leads to the energy gain $\Delta E \simeq (-19.50 + 6\pi)\kappa \simeq -0.65\kappa$. For $\gamma > 0$, the energy gain ΔE results from the differences of the total energies E obtained by integration of the whole energy densities, because the energy densities slightly differ also for $z/r_m > 0$.

The vanishing energy gain in Fig. 5a for large values of the rescaled adhesion energy u and reduced potential ranges with $\xi = 0.5$ nm and $\xi = 0.25$ nm can be understood by comparing the total energy densities e for the finite minimum value $r_n = 2.5$ nm of the neck radius (full lines in Fig. S3) to total energy densities with unconstrained neck radii as in Ref. 1 (dashed lines in Fig. S3). For the minimum neck radius $r_n = 2.5$ nm, the minima of the total energy densities at $\xi = 0.5$ nm and 0.25 nm are shifted to smaller values of z/r_m, compared to the profiles for unconstrained necks. An integration of the energy densities for the minimum neck radius $r_n = 2.5$ nm leads to the values $\Delta E \simeq -0.65\ \kappa$, $-0.25\ \kappa$, and $0.04\ \kappa$ for $\xi = 1$ nm, 0.5 nm, and 0.25 nm, respectively. The positive ΔE value for $\xi = 0.25$ nm implies that the interplay of bending and adhesion energies in the contact regions at which the membrane detaches from the particles in necks is no longer favourable, compared to a corresponding spherical membrane segment r_m for an individually wrapped particle. An integration of the energy densities for unconstrained necks leads to the values $\Delta E \simeq -0.65\ \kappa$, $-0.29\ \kappa$, and $-0.14\ \kappa$ for $\xi = 1$ nm, 0.5 nm, and 0.25 nm, respectively. The resulting neck radii $r_n = 1.51$ nm and 0.80 nm for $\xi = 0.5$ nm, and 0.25 nm, however, are unrealistically small. For $\xi = 1$ nm, the membrane profiles are not affected by the minimum value 2.5 nm of the neck radius, because the resulting neck radius $r_n = 2.95$

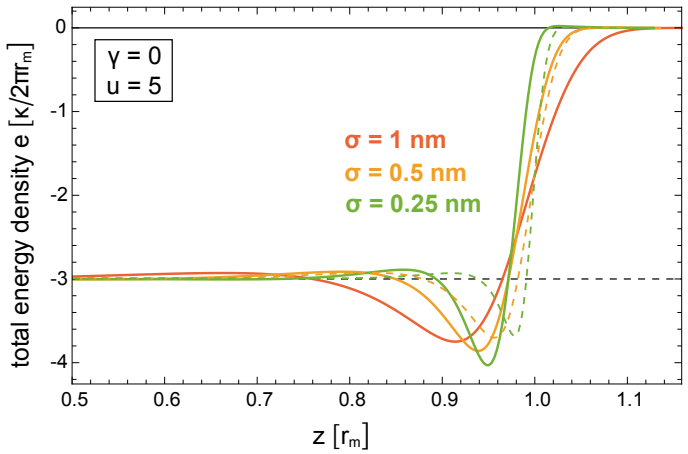

Fig. S3 Total energy densities e of a central particle in a tubule in the contact region with rescaled coordinate z/r_m for a minimum neck radius $r_n = 2.5$ nm (full lines) and for unconstrained membrane necks (dashed lines) of tensionless membranes at the rescaled adhesion energy $u = 5$ as in Fig. 5 and at different values of the standard deviation ξ of the Gaussian adhesion potential.

nm is larger than this minimum value at which the neck is closed.

Data availability

All Mathematica 14.3 notebooks used to generate and plot the data of this article are available in the open research data repository Edmond at https://doi.org/10.17617/3.OAPOLZ[6].

References

1 M. Raatz, R. Lipowsky and T. R. Weikl, *Soft Matter*, 2014, **10**, 3570–3577.

2 Wolfram Research, Inc., *Mathematica, Version 14.3*, `https://www.wolfram.com/mathematica`, Champaign, IL, 2025.

3 T. R. Weikl, M. M. Kozlov and W. Helfrich, *Phys. Rev. E*, 1998, **57**, 6988–6995.

4 R. Groza, K. V. Schmidt, P. M. Müller, P. Ronchi, C. Schlack-Leigers, U. Neu, D. Puchkov, R. Dimova, C. Matthaeus, J. Taraska, T. R. Weikl and H. Ewers, *Nat. Commun.*, 2024, **15**, 2767.

5 G.-K. Xu, J. Hu, R. Lipowsky and T. R. Weikl, *J. Chem. Phys.*, 2015, **143**, 243136.

6 T. Weikl, *Mathematica notebooks for article "Membrane tubulation by spherical nanoparticles: Effect of lateral tension"*, 2026, `https://doi.org/10.17617/3.OAPOLZ`.